Boron Chemistry

DOI: 10.1002/anie.201001275

B_{19}^-: An Aromatic Wankel Motor**

J. Oscar C. Jiménez-Halla, Rafael Islas, Thomas Heine, and Gabriel Merino**

Recently, Huang et al. found that the lowest energy form of B_{19}^- (**1**) is a beautiful ring structure with two planar π-aromatic systems nested inside one another.[1] The inner fragment (ring A) is a pentagonal six-atom group sharing two π electrons, surrounded by a peripheral layer of thirteen boron atoms (ring B), sharing further ten π electrons (Figure 1). Interestingly, both fragments individually satisfy the $(4n+2)\pi$ Hückel aromaticity rule. In general, the structures of neutral and anionic clusters ranging from B_3 to B_{20} adopt planar geometries rather than three-dimensional cluster structures, and in most cases are doubly aromatic.[2] Particularly, B_8^{2-}, B_9^-, B_{10}, B_{11}^-, B_{12}, and B_{13}^+ boron clusters can be considered as all-boron analogues of benzene.[3–7] However, B_{19}^- is different, even when concentric π systems have been reported in organic chemistry before, none has exactly this electronic configuration.

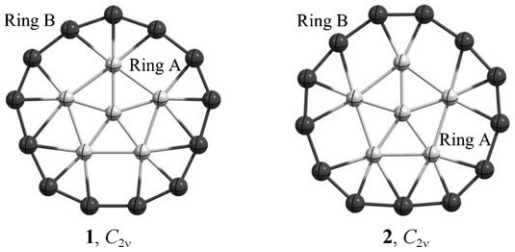

Figure 1. Geometries of the global minimum **1** and the transition state **2** of B_{19}^- related to the synchronized rotation of ring A (light spheres) and ring B (dark spheres).

In the last ten years, several boron wheels with main-group elements[8–14] or transition-metal atoms[15–18] at the ring center have been proposed theoretically. In 2005, Erhardt et al. studied some aromatic boron wheels (C_2B_8, $C_3B_9^{3+}$, and $C_5B_{11}^+$) with more than one carbon at the center (Figure 2).[19]

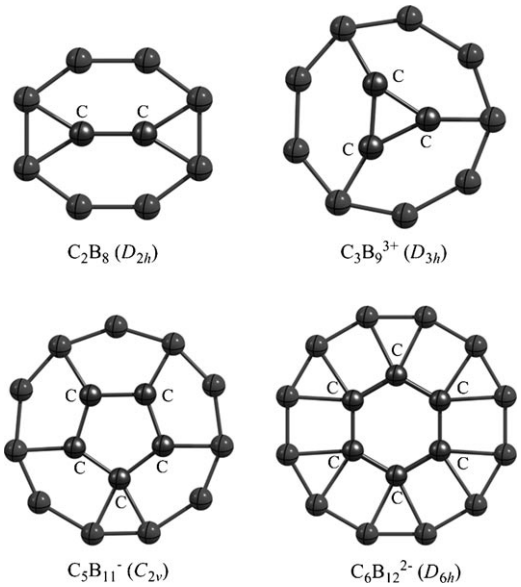

Figure 2. Structures of the aromatic borocarbon wheels reported by Erhardt et al.[19] and Wu et al.[10]

They found that the carbon fragment is enclosed by a peripheral ring made by a suitable number of boron atoms. It is remarkable that the inner carbon fragments and the outer boron rings can rotate almost freely in opposite directions. The rotational barriers are 2.6, 0.7, and 0.1 kcal mol^{-1} for C_2B_8, $C_3B_9^{3+}$, and $C_5B_{11}^+$, respectively, calculated at the B3LYP/6-311+G(d) level. A similar situation occurs in $C_6B_{12}^{2-}$.[10] Unfortunately, in all these borocarbon wheels, isomers with carbon atoms on the outside are lower in energy. In fact, carbon does not like to be placed at the center of a boron wheel as described recently by Boldyrev and Wang.[14,20,21]

It is important to note that in gas-phase methods, where clusters are produced in thermally excited conditions, the mixture of products is governed by the thermodynamics.[22] For clusters, in most cases, only one isomer—the global minimum—is formed as the product. This result has been confirmed in experiment and theory by Wang and Boldyrev in various studies for a series of related systems.[1,3,4,14] In consequence, it will be impossible to produce the borocarbon

[*] Dr. J. O. C. Jiménez-Halla, R. Islas, Prof. Dr. G. Merino
Departamento de Química, División de Ciencias Naturales y Exactas
Universidad de Guanajuato. Col. Noria Alta s/n
36050 Guanajuato (Mexico)
Fax: (+52) 4737-320006
E-mail: gmerino@quijote.ugto.mx
Prof. Dr. T. Heine
School of Engineering and Science
Jacobs University Bremen, 28759 Bremen (Germany)
Fax: (+49) 421-200-493-223
E-mail: t.heine@jacobs-university.de

[**] Financial support from the Air Force Research Laboratory Latin American Initiative Project and DAIP-UGTO are acknowledged. R.I. thanks CONACYT for a Ph.D. fellowship. We also thank to Prof. Miquel Solà and Prof. Miguel A. García-Garibay for their useful comments and discussions.

Supporting information for this article is available on the WWW under http://dx.doi.org/10.1002/anie.201001275.

clusters proposed earlier in thermodynamically governed experiments.

So, our main question is whether **1**, a global minimum structure, also shows the fluxional behavior discussed by Erhardt et al. To answer this question, we have carried out a careful theoretical investigation, where we located the transition state of the rotation of the two boron rings with respect to each other, and by studying the fluxionality of the system using Born–Oppenheimer molecular dynamics (BO-MD) calculations. We also analyzed in detail the aromatic properties of **1** using the induced magnetic field ($\mathbf{B}^{ind}$).[23,24]

The first insight about the dynamic independence of rings A and B is given by the harmonic analysis. The geometry of **1** has been optimized at the B3LYP/6-311 + G(d) level, leading to a planar structure of point group C_{2v}.[25]

The vibrational analysis demonstrates that **1** is a minimum, and the smallest vibrational frequency corresponds to a soft mode of 60 cm^{-1} and is assigned to the rotation of the inner boron ring A. Following the smallest frequency mode leads to the transition state, **2**, which also has C_{2v} symmetry, of the ring rotation **1**→**2**→**1′** (its smallest frequency is 59*i* cm^{-1}).[26] The energy difference between **1** and **2** is negligible (less than 0.1 kcal mol^{-1}), indicating a quasi free rotation of the inner boron ring.

The relative energies of B_{19}^- isomers have been studied by Huang et al. They optimized the structures at the B3LYP/6-311 + G(d) level and substantiated the relative energies by single-point CCSD(T)/6-311 + G(d) calculations. Interestingly, at this level they find that the global minimum structure has C_s symmetry, but after zero-point vibrational energy (ZPVE) correction the structurally and energetically very similar C_{2v} isomer, **1**, is more stable. As the difference of the ZPVE exceeds the energy difference between both isomers, we can speak of a vibrationally averaged structure. We used the data of Huang et al. for **1** as the starting geometry for our investigations.

We also found the transition state that was obtained by Huang et al. for the isomerization of **1** to the closest energy structure **4** (Figure 3). The energy difference between **1** and **4** is 2.8 kcal mol^{-1}, and the isomerization barrier is 22.7 kcal mol^{-1}, precluding this change at low temperatures. To maintain the integrity of the outer boron ring during the transformation, note that the transition state **3** is not planar (205*i* cm^{-1}).

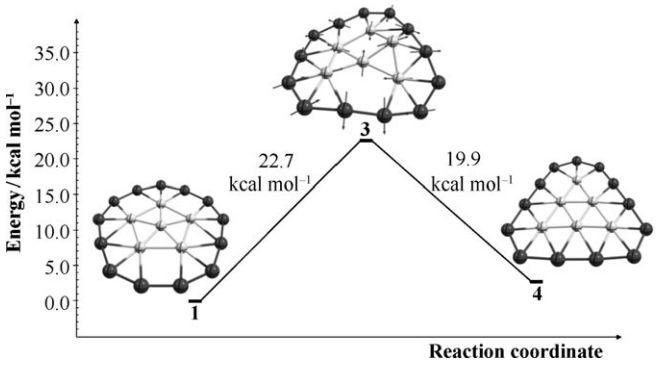

Figure 3. Isomerization of **1** to the next lowest in energy species **4**, calculated at the B3LYP/6-311 + G(d) level.

BO–MD simulations at the PBE/DZVP-GGA level[27] support the fluxional behavior. The simulation was started from the equilibrium geometry **1**, with random velocities assigned to the atoms, and the structure was equilibrated for 300 and 600 K, employing a Nosé–Hoover thermal bath, for 20 ps. Then, 60 ps trajectories were calculated. During the BO–MD simulations, the molecule essentially maintains its planar geometry, and internal and external rings rotate nearly freely with respect to each other. The fluxional behavior of **1** is already indicated in its equilibrium structure: each boron atom of the inner pentagonal wheel is coordinated to three atoms of the outer wheel. However, some of these bonds between ring A and ring B are exclusive (that is, they are the only bond formed by the boron atom in ring B to a boron atom in ring A), and some ring B atoms form two bonds to ring A atoms. This arrangement results in an interruption of the rather regular pattern of triangles by three squares, so the internal pentagon is neighbored by three squares and two triangles. A rotation follows then a simple mechanism, which is indicated by the transition state **2**: A slight motion of an atom of the inner pentagon towards the center of a square results in the formation of a new bond across the diagonal of the square. The bond strengthens, and the atom is pulled further towards the center of the square. In consequence, the bond between one boron and ring B is stretched and eventually broken, and a new square is created, leading to a topology as in the equilibrium structure, but with the individual atoms at different positions. Note that the pentagonal ring of **1** needs to turn by only 13.8° to be transformed into the transition state **2**.[28] In summary, B_{19}^- could be considered the first molecular cluster behaving like a "Wankel engine".

Of course, the bonding situation of this aromatic boron cluster is intriguing. In this sense, Huang et al. studied the bonding properties of **1** in detail using the adaptive natural density partitioning (AdNDP) analysis and showed that a strong delocalization of the σ and π system is present in **1**.[1] However, there are some details about aromaticity that were not explored and could give some insight about the fluxional behavior of **1**.

The NMR-spectrum calculations at the PW91/IGLO-III level employing the GIAO method reveal that the ^{11}B NMR chemical shifts[29] change strongly from the boron atoms in the inner ring to those in the outer. The central atom has a value of $\delta = -40.1$ ppm. The boron atoms in ring A are more shielded by $\delta = 20$ ppm compared to the central atom, while chemical shifts of boron ring B range from $\delta = -17$ to 37 ppm.

Figure 4 shows the diatropic isolines of the *z*-component of the induced magnetic field, B^{ind}_z, for an external field applied perpendicular to the molecular plane of **1**.[23] A magnetic field in this direction can induce a ring current in, and parallel to, the molecular plane. The total magnetic response, which is mathematically equal to $NICS_{zz}$, shows a long-range shielding cone perpendicular to the molecular plane. This cone is even more intense than that observed in benzene. Note that ring A lies in the strong shielding area (approximately 100 ppm) of the induced field. The B^{ind}_z

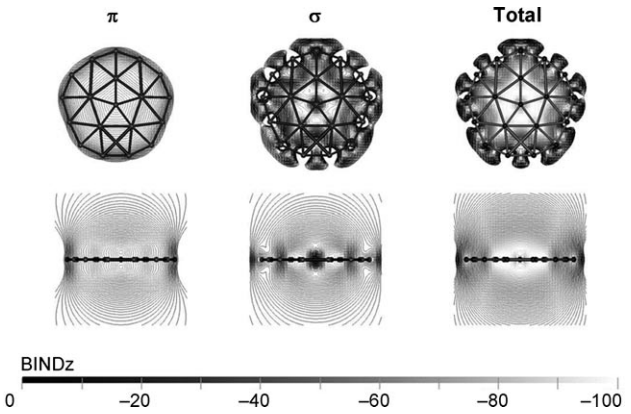

Figure 4. The diatropic region of B^{ind}_z for **1** calculated at the PW91/IGLO-III level using the IGLO method, shown in the molecular plane (top) and perpendicular to it (bottom).

intensity diminishes gradually from the inner to the outer ring B, confirming the presence of two concentric π rings.

As our method allows the separation into core, σ, and π orbitals, we can discuss the role of each contribution.[30] The core electrons do not contribute to $\mathbf{B}^{ind}$ except in the very close vicinity of nuclei. Interestingly, the local diamagnetic contributions of the σ electrons generate a long-range response and a diatropic (shielding) region in the pentagonal ring.

Furthermore, the π-orbital contribution shows the typical response of an aromatic system. The field lines parallel to the molecular plane lose the shape of the molecular framework and become circles. No paratropic (deshielding) contributions are found inside the ring. Outside the molecule, the field lines form long-range cones (shielding cones). The π contributions are, however, smaller in magnitude than those of the σ skeleton, which results in a strong total response. So, similar to Al_4^{2-},[31,32] the contribution of the π system in **1** is smaller than that of the σ-system, but it is still important for the total response. In this sense, B_{19}^- is a double aromatic system.

The B^{ind}_z isolines of **2** indicate essentially the same magnetic response in shape and intensity as **1**. Thus, during the rotation, the changes in σ and π aromaticity are negligible. This is a big difference to classical organic systems, such as coronene, where the rotation of the inner ring modifies drastically the overlap of the π system and thus aromaticity.

Comparison between **1** and the system reported earlier by Erhardt et al. (see Figure 2) clearly shows that the rotational barrier depends on the size of the external wheel. The correct size decreases the overlap between rings A and B, allowing a quasi-free rotational movement. But this essentially barrier-free rotation depends also on the electronic structure, as proper σ- and π-electron delocalization is maintained at both the minimum and transition state (**1** and **2**). Note that during the rotations, the multicenter B–B binding interactions transform gradually from one arrangement to the other, and that the same B–B contacts exist in the transition states and in the minima.

The dynamic behavior of B_{19}^- is evident from the BO–MD simulations, which indicate motions which are similar to those of a Wankel motor. Further study to find other fluxional boron clusters is underway.

Received: March 2, 2010
Revised: April 21, 2010
Published online: July 6, 2010

Keywords: aromaticity · boron · concentric π systems · density functional calculations · molecular dynamics

[1] W. Huang, A. P. Sergeeva, H. J. Zhai, B. B. Averkiev, L.-S. Wang, A. I. Boldyrev, *Nat. Chem.* **2010**, *2*, 202–206.
[2] D. Y. Zubarev, A. I. Boldyrev, *J. Comput. Chem.* **2007**, *28*, 251–268.
[3] H. J. Zhai, A. N. Alexandrova, K. A. Birch, A. I. Boldyrev, L.-S. Wang, *Angew. Chem.* **2003**, *115*, 6186–6190; *Angew. Chem. Int. Ed.* **2003**, *42*, 6004–6008.
[4] A. N. Alexandrova, H. J. Zhai, L.-S. Wang, A. I. Boldyrev, *Inorg. Chem.* **2004**, *43*, 3552–3554.
[5] P. W. Fowler, B. R. Gray, *Inorg. Chem.* **2007**, *46*, 2892–2897.
[6] H. J. Zhai, B. Kiran, J. Li, L.-S. Wang, *Nature Mater.* **2003**, *2*, 827–833.
[7] J. E. Fowler, J. M. Ugalde, *J. Phys. Chem. A* **2000**, *104*, 397–403.
[8] B. B. Averkiev, A. I. Boldyrev, *Russ. J. Gen. Chem.* **2008**, *78*, 769–773.
[9] K. Exner, P. von R. Schleyer, *Science* **2000**, *290*, 1937–1940.
[10] Y. B. Wu, C. X. Yuan, P. Yang, *J. Mol. Struct. (THEOCHEM)* **2006**, *765*, 35–38.
[11] R. Islas, T. Heine, K. Ito, P. von R. Schleyer, G. Merino, *J. Am. Chem. Soc.* **2007**, *129*, 14767–14774.
[12] J. M. Xiong, L. F. Gong, Q. S. Li, *Chem. J. Chin. Univ.* **2007**, *28*, 1968–1971.
[13] Y. Pei, X. C. Zeng, *J. Am. Chem. Soc.* **2008**, *130*, 2580–2592.
[14] B. B. Averkiev, L. M. Wang, W. Huang, L.-S. Wang, A. I. Boldyrev, *Phys. Chem. Chem. Phys.* **2009**, *11*, 9840–9849.
[15] K. Ito, Z. Pu, Q. S. Li, P. von R. Schleyer, *Inorg. Chem.* **2008**, *47*, 10906–10910.
[16] J. C. Guo, W. Z. Yao, Z. Li, S. D. Li, *Sci. China Ser. B* **2009**, *52*, 566–570.
[17] C. Q. Miao, J. C. Guo, S. D. Li, *Sci. China Ser. B* **2009**, *52*, 900–904.
[18] Z. F. Pu, K. Ito, P. von R. Schleyer, Q. S. Li, *Inorg. Chem.* **2009**, *48*, 10679–10686.
[19] S. Erhardt, G. Frenking, Z. F. Chen, P. von R. Schleyer, *Angew. Chem.* **2005**, *117*, 1102–1106; *Angew. Chem. Int. Ed.* **2005**, *44*, 1078–1082.
[20] B. B. Averkiev, D. Y. Zubarev, L. M. Wang, W. Huang, L.-S. Wang, A. I. Boldyrev, *J. Am. Chem. Soc.* **2008**, *130*, 9248–9250.
[21] L. M. Wang, W. Huang, B. B. Averkiev, A. I. Boldyrev, L.-S. Wang, *Angew. Chem.* **2007**, *119*, 4634–4637; *Angew. Chem. Int. Ed.* **2007**, *46*, 4550–4553.
[22] Z. Slanina, S. L. Lee, F. Uhlik, L. Adamowicz, S. Nagase, *Theor. Chem. Acc.* **2007**, *117*, 315–322.
[23] G. Merino, T. Heine, G. Seifert, *Chem. Eur. J.* **2004**, *10*, 4367–4371.
[24] G. Merino, A. Vela, T. Heine, *Chem. Rev.* **2005**, *105*, 3812–3841.
[25] We have used the Gaussian03 rev. D.02 computational package (M. J. Frisch, et al. Gaussian Inc.: Pittsburgh, PA, **2003**) for performing this part of the analysis. Similar geometrical and energetic results have been obtained at the PBE/6-311+G(d) level. All the optimized geometries are given in the Supporting Information.

[26] We have ensured that this transition state connects truly to both minima on each side by performing an IRC calculation at this level.
[27] The deMon program package (A. M. Köster, et al. *deMon2k*, The deMon Developers Community, Mexico, **2008**) was used for such calculations.; a) B. Hammer, L. B. Hansen, J. K. Norskov, *Phys. Rev. B.* **1999**, *59*, 7413 – 7421; b) P. Calaminici, F. Janetzko, A. M. Köster, R. Mejia-Olvera, B. Zuniga-Gutierrez, *J. Chem. Phys.* **2007**, *126*, 044108.
[28] A video clip of this trajectory is available at http://quimera.ugto.mx/qtc/b19.html and at http://www.youtube.com/watch?v=Dj7-4NjowiQ.
[29] These values are denoted with respect to $BF_3{\cdot}OEt_2$.
[30] T. Heine, R. Islas, G. Merino, *J. Comput. Chem.* **2007**, *28*, 302 – 309.
[31] A. I. Boldyrev, L.-S. Wang, *Chem. Rev.* **2005**, *105*, 3716 – 3757.
[32] R. Islas, T. Heine, G. Merino, *J. Chem. Theory Comput.* **2007**, *3*, 775 – 781.

